

Magnetic Properties of Lanthanum Orthoferrites Containing Lattice Defects

HIROSHI YAMAMURA, SHIN-ICHI SHIRASAKI, HIROTOSHI OSHIMA

National Institute for Researches in Inorganic Materials, Kurakake, Sakura-Mura, Niihari-Gun, Ibaraki, Japan

AND KAZUYUKI KAKEGAWA

Faculty of Engineering, Chiba University, Yayoi-Cho, Chiba, Japan

Received February 17, 1976; in revised form April 16, 1976

Polycrystalline lanthanum orthoferrites were prepared by firing coprecipitated hydroxides of La^{3+} and Fe^{3+} at elevated temperatures. The materials fired at temperatures below 1100°C were characterized by the coexistence of such lattice vacancies that the concentration ratio of $V_{\text{La}}:V_{\text{Fe}}:V_{\text{O}}$ is always equal to that of the constituent atoms of LaFeO_3 . They exhibited a large magnetic susceptibility, a low Néel temperature, and a small spontaneous magnetization, in comparison with lanthanum orthoferrite without these vacancies. These characteristics originated essentially from a local reduction in anisotropic superexchange interaction at vacant sites. The lowering of Néel temperature characteristic of these materials was interpreted in terms of a decrease in the number of $\text{Fe}^{3+}\text{-O-Fe}^{3+}$ linkages due to the existence of oxygen and iron vacancies.

Introduction

Among many materials that exhibit a parasitic ferromagnetism (or a weak ferromagnetism) (1, 2) there is an orthoferrite family, $R\text{FeO}_3$ where R is La and other rare-earth elements (3). The space group of LaFeO_3 has been determined as $Pbnm(D_{2h}^{16})$ by Geller and Wood (4). This structure is a distorted perovskite with four equivalent iron ions per unit cell. Neutron diffraction has indicated that each Fe^{3+} ion is surrounded by six Fe^{3+} neighbors whose spins are alternately antiparallel (G-type structure) (5). Belov *et al.* (6) have observed magnetic thermoresidual behavior in a lanthanum orthoferrite family where Fe^{3+} ions were partially replaced with other trivalent ions.

Polycrystalline lanthanum orthoferrite usually can be prepared by solid-state reaction of an intimate mixture of La_2O_3 and Fe_2O_3 at

elevated temperatures. In the present study, La^{3+} and Fe^{3+} ions were coprecipitated from aqueous solution by the addition of NH_4OH solution, followed by heat treatment to obtain lanthanum orthoferrites. The main purpose of the present study is to show the possible existence of metastable vacancies in the materials prepared in this way and then to correlate their magnetic properties with such defect structures of lanthanum orthoferrites.

Sample Preparation and Experimental Procedure

Guaranteed reagent $\text{Fe}(\text{NO}_3)_3 \cdot 9\text{H}_2\text{O}$ (Kanto Chemicals Co.) and La_2O_3 (Shin-etsu Chemicals Co.) were used as starting materials. The Fe content in $\text{Fe}(\text{NO}_3)_3 \cdot 9\text{H}_2\text{O}$ was chemically analyzed, and La_2O_3 was heated at about 1000°C because it is hygroscopic. La_2O_3 and $\text{Fe}(\text{NO}_3)_3 \cdot 9\text{H}_2\text{O}$ were weighed out

so as to have La/Fe atomic ratio = 1.0 and then dissolved in weakly acidic water. The mixed solution was heated to about 80°C and then added to a concentrated aqueous NH₄OH solution with thorough stirring. The resultant precipitates were decanted with water several times, filtered, and then oven-dried overnight at 120°C. The dried precipitates were fired at various temperatures between 500 and 1200°C, and each for 2 hr in air.

The 1200°C-fired material was analyzed chemically for La and Fe. The La content was determined gravimetrically in the form of La₂O₃. The Fe content was determined by titration using potassium permanganate.

X-ray diffraction examinations were carried out to define the phases using CuK α radiation and silicon powder as a standard material. It is generally known that X-ray diffraction lines of solids broaden for very small crystallite size and/or the presence of lattice strain. To investigate the origin of diffraction lines broadening in the materials, fluctuation of the interplanar spacing, $\Delta d/d$, was calculated by observing the diffraction angle, 2θ , and pure diffraction line broadening, β , relative to α -SiO₂ as standard and using the equation $\Delta d/d = \beta \cos \theta / \sin \theta$. The crystallite size was determined simultaneously using the same equation. Each K α ₁ and K α ₂ diffraction doublet was separated according to Jones's method (7).

The density of the fired materials was determined as a function of firing temperature, according to Cabri's method (8). Each finely divided sample was immersed in distilled water, the temperature of which was held at 27°C by means of a water bath equipped with a temperature controller. A difference between the respective weights in air and in water was measured, and the buoyancy, the volume of the samples, and then the density were determined.

Magnetic susceptibility and magnetization were measured using a Faraday-type magnetic balance (Shimadzu Co.). The measurements were carried out between room temperature and 600°C. The magnetic susceptibility was estimated from the slope of the straight line of magnetization vs magnetic field. The magnitude of parasitic ferromagnetism can be regarded as magnetization where magnetic

field = 0.0. Paramagnetic Mohr's salt and Co[Hg(SCN)₄], the susceptibilities of which are 32.6×10^{-6} and 16.4×10^{-6} emu/g at 20°C, respectively, were used as standard materials.

Mössbauer spectra were taken by use of a spectrometer (Elscent Co.) operated in constant acceleration mode. Iron foil was used as standard and the source was ⁵⁷Co dispersed in copper. The velocities, in millimeters per second, are taken relative to metallic iron.

Results and Discussion

Characterization of the Materials

The results of chemical analyses for La and Fe in the chemically precipitated material are given in Table I. The La content was somewhat less than that in LaFeO₃. The compositional formula was conveniently written as La_{0.963}FeO_{2.945} (or 0.963 La₂O₃·Fe₂O₃), assuming iron is trivalent.

It was seen by means of thermal gravimetry that the weight change continued almost up to 700°C. To avoid confusion, therefore, we studied especially the properties of the materials heat-treated above 700°C.

No X-ray diffraction was observed for the precipitate fired at 500°C. When the precipitate was fired at temperatures between 600 and 700°C, cubic perovskite resulted, with X-ray diffraction lines that were weak and broad. In view of the fact that parasitic ferromagnetism was observed in these materials (as described later), the materials do not seem to be exactly cubic, since parasitic ferromagnetism cannot appear in cubic crystals in general. Elevation of the firing temperature made the diffraction lines strong and sharp. There was no evidence

TABLE I
CHEMICAL ANALYSIS OF LaFeO₃

	Fe ₂ O ₃	La ₂ O ₃
Observed value (wt %)	33.4	65.9
Calculated value (wt %)	32.9	67.1
Atomic ratio	1	0.963

of "impurity phases" such as La_2O_3 , Fe_2O_3 , or $\text{La}_3\text{Fe}_5\text{O}_{12}$ in the materials, so far as X-ray diffraction measurements were concerned. In a firing temperature range between 800 and 1000°C, orthorhombic perovskite resulted. Firing at temperature above 1000°C produced GdFeO_3 -type LaFeO_3 with orthorhombic symmetry. Upon firing at 1200°C, the lattice constants were $a = 5.555$, $b = 5.560$, and $c = 7.859$ Å, very close to the previously reported data of "pure" LaFeO_3 ($a = 5.556$, $b = 5.565$, $c = 7.862$ Å) (4). Figure 1 shows the lattice constant as a function of the firing temperature, where cubic symmetry is assumed for convenience.

Mössbauer spectra taken at room temperature of the materials heat-treated at 500, 700, and 1200°C are shown in Fig. 2. For specimen 500 (i.e., the material heat-treated at 500°C in air), which was found to be amorphous by X-ray diffractometer, the spectrum indicated the presence of paramagnetic iron for which the isomer shift and the quadrupole splitting were +0.215 and 0.484 mm/sec, respectively (Fig. 2a). For specimen 700 magnetic hyperfine splitting resulted and the absorption lines were very diffuse (Fig. 2b). The observed isomer shift and the magnetic field for the material were +0.447 mm/sec and 521 kOe, respectively. The corresponding Mössbauer parameters for specimen 1200 are, respectively, +0.373 mm/sec and 526 kOe, both of which agree well with our previous data on LaFeO_3 prepared by the solid-state reaction method (9) (Fig. 2c). The values of the isomer shift indicate that the iron atoms are trivalent for all the specimens. It was confirmed that the

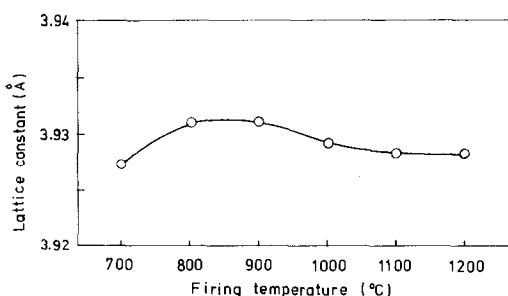


FIG. 1. Lattice constant as a function of firing temperatures.

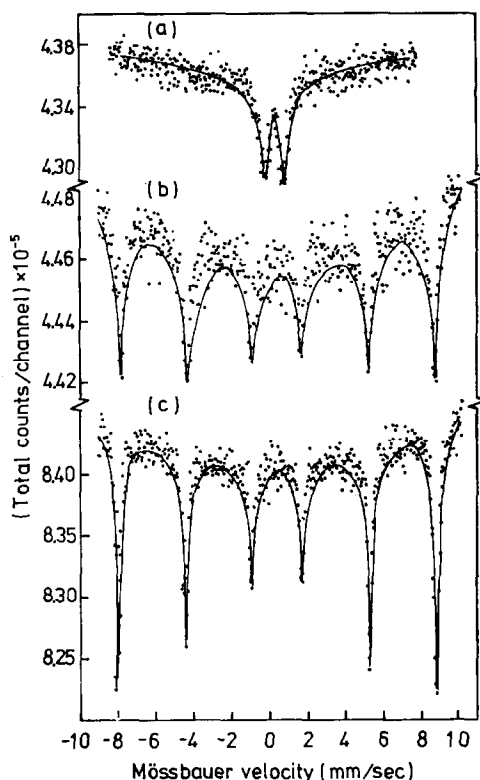


FIG. 2. Mössbauer spectra of LaFeO_3 heat-treated (a) at 500°C, (b) at 700°C, and (c) at 1200°C in air.

half-height width of the absorption lines decreased as firing temperature increased. This suggests the existence of defects in the materials fired at lower temperatures.

The density of these materials is given in Table II. The calculated density, 6.49 g/cm^3 , of specimen 1200 agreed well with the observed value, $6.51 \pm 0.02 \text{ g/cm}^3$. On the other hand, the density of "pure" LaFeO_3 was estimated to be 6.63 g/cm^3 . This disagreement would originate from the lanthanum deficiency. The observed density of the materials was smaller than 6.49 g/cm^3 , the value of specimen 1200. It should be emphasized that all the materials concerned were monophasic to X-ray diffractometry and had the same atomic ratio of La/Fe ($= 0.963$). To interpret the firing temperature dependence of density reliably, it seems reasonable to assume the existence of vacancies such that the vacancy concentration ratio of $V_{\text{La}} : V_{\text{Fe}} : V_{\text{O}}$ is always equal to that of

TABLE II
CHARACTERISTIC DATA FOR LANTHANUM ORTHOFERRITE SERIES
CONTAINING LATTICE DEFECTS

Firing temperature (°C)	Crystallite size (Å)	$(\Delta d/d) \times 10^3$	ρ_{obs} (g/cm ³)	Vacancy concentration (x)
700	400	5.57	5.813 ± 0.02	0.107
800	510	2.46	6.060	0.069
900	600	1.55	6.197	0.048
1000	770	1.38	6.391	0.019
1100	—	—	6.512	~ 0
1200	1090	1.22	6.513	~ 0

the constituent atoms of LaFeO₃ for the materials fired at lower temperatures. We therefore propose a formula La_{0.963(1-x)}Fe_(1-x)O_{2.945(1-x)} for the materials. The *x* value, which is the vacancy concentration, can be determined using the following equation,

$$\frac{\text{La}_{0.963(1-x)}\text{Fe}_{(1-x)}\text{O}_{2.945(1-x)}}{U_o \times 10^{-24} \times 6.02 \times 10^{23}} = \rho_{obs},$$

where U_o and ρ_{obs} are the unit volume (Å³) and the observed density, respectively. The results are given in the last column of Table II. The *x* value decreases with increasing firing temperature. In this view, the vacancies of interest may be regarded as metastable ones. It is noted that these materials containing vacancies were characterized by X-ray diffraction line broadening. The crystallite size and the degree of fluctuation of interplanar spacing, $\Delta d/d$, are summarized as functions of the firing temperature in Table II. The firing-temperature elevation is followed by an increase of the crystallite size and by a decrease of the $\Delta d/d$ value. It seems likely that the presence of vacancies causes an increase of $\Delta d/d$ value. This value can be seen as a parameter of either inhomogeneous strain or compositional fluctuation in these materials. The constituent atoms in the materials which were crystallized at fairly low temperatures would be located away from the potential minimum site. When the firing temperature so increases that the potential barrier could be overcome, they diffuse to regular position, and then the vacancy concentration and $\Delta d/d$ decrease.

Magnetic Properties

As shown in Fig. 3a, the Mössbauer spectra exhibit the presence of paramagnetic iron for the amorphous material, and the magnetic susceptibility (χ_g) of the antiferromagnetic materials decreases with firing-temperature elevation (Table III). The large χ_g of the poorly crystallized materials would originate from the disordering of the spins with antiferromagnetic interactions. Specimen 1200 exhibited parasitic ferromagnetism ($\sigma_o = 0.018$ emu/g), whereas no other materials had a ferromagnetic moment at room temperature. The magnitude of the magnetization of the materials showed sharp maximums in the vicinity of their Néel temperatures, the extent of the sharpness depending on the thermal histories. The temperature dependence of magnetization in a field of 11.6 kOe for a typical specimen 800 is shown in Fig. 3. To clarify the reason why a magnetization maximum appears with rising temperature, the values of both χ_g and σ_o at various temperatures were separately estimated. The results are shown in Fig. 3, where the hatched part is for the σ_o value and the nonhatched part, for the χ_g value. The σ_o value comes out from 256°C and increases with increasing temperature. The χ_g value also increases with an increase of temperature, showing a maximum near the Néel temperature. To study the temperature-dependence behavior of both χ_g and σ_o in more detail, the relative magnetic susceptibility, $\chi_g/\chi_g(T_N)$, and the relative spontaneous magnetization, $\sigma_o/\sigma_o(T_N)$, were

TABLE III
MAGNETIC DATA FOR LANTHANUM ORTHOFERRITE SERIES
CONTAINING LATTICE DEFECTS

Firing temperature (°C)	$\chi_\theta^a \times 10^6$ (emu/g)	σ_o^a (emu/g)	T_N (°C)	$\chi_\theta^b \times 10^6$ (emu/g)	σ_o^b (emu/g)
700	16.45	0	397	17.5	0.235
800	9.85	0	431	12.8	0.314
900	9.35	0	447	11.8	0.425
1000	8.80	0	450	11.5	0.505
1100	8.90	0	452	11.3	0.530
1200	8.70	0.018	452	11.7	0.563

^a The value of the as-fired materials.

^b The value after the material was cooled in a magnetic field.

calculated and plotted as functions of the reduced temperature, T/T_N (Fig. 4). As seen, no firing-temperature dependence of the value of $\chi_\theta/\chi_\theta(T_N)$ was recognized, whereas the value of $\sigma_o/\sigma_o(T_N)$ varied with the firing temperature of the materials. The firing-temperature dependence of magnetization is, therefore, based on the firing-temperature dependence of σ_o , which varies from one sample to another. When the materials were fired at lower temperature, the spontaneous magnetization started from a lower temperature (Fig. 4).

When these materials were cooled from the Néel temperature down to room temperature in the same magnetic field, a large magnetization resulted compared with the case of the rising-temperature procedure. From the

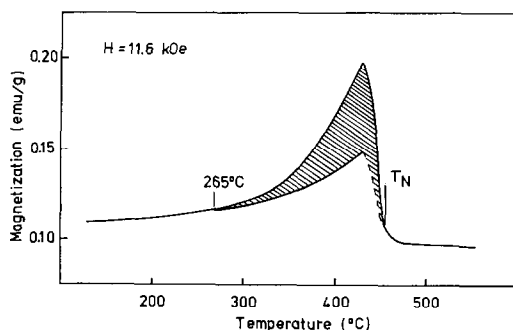


FIG. 3. Magnetization vs temperature of LaFeO_3 heat-treated at 800°C in air. The hatched part is for the σ_o value and nonhatched part, for the χ_θ value.

measurements of magnetization as a function of magnetic field at various temperatures, such a high degree of magnetization was found to originate from a parasitic ferromagnetic moment that appeared additively in the cooling procedure. Thus, we can see this behavior as thermoresidual magnetization that is able to appear when a single-domain grain of parasitic ferromagnet is cooled through Néel temperature (6).

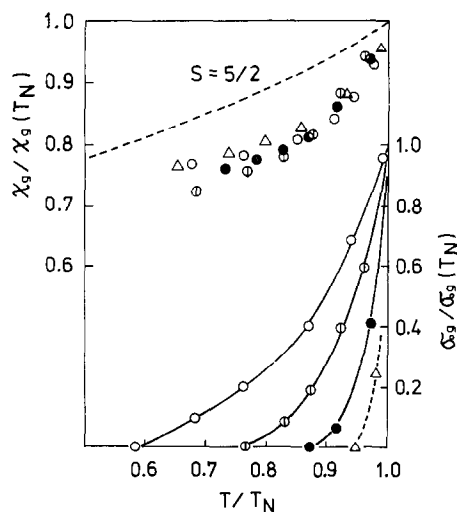


FIG. 4. Relative magnetic susceptibility ($\chi_\theta/\chi_\theta(T_N)$) and relative spontaneous magnetization ($\sigma_o/\sigma_o(T_N)$) as a function of reduced temperature (T/T_N) for the specimens fired at 700°C (\circ), 800°C (\odot), 900°C (\bullet) and 1000°C (Δ).

The magnetic data of lanthanum orthoferrites containing vacancies are summarized in Table III, where T_N is the temperature at which the thermoresidual magnetization disappears. The T_N value agreed with that obtained from the temperature dependence of the internal magnetic field in the Mössbauer spectra. The T_N value of specimen 1200, for example, was found to be 452°C, being slightly lower than Treves's value, 465°C (10). These values fit those obtained from magnetization measurements well. A decrease in the firing temperature was followed by a decrease of both T_N and thermoresidual magnetization. Gilleo (11) in his study of superexchange interaction of various oxides indicated that the T_N depends primarily upon the number of $\text{Fe}^{3+}\text{-O-Fe}^{3+}$ linkages. It is thus expected that the presence of lattice vacancies reduces the number of $\text{Fe}^{3+}\text{-O-Fe}^{3+}$ linkages and therefore the T_N value. For n interactions per magnetic ion per formula unit (i.e., the average number of interactions per magnetic ion), the interaction energy, J , would be expected to be proportional to T_N/n (12). Gilleo further showed that an average value of T_N/n was 115° with extremes of 106° and 132° for various iron oxides, and that the strength of the exchange interaction increased as the $\text{Fe}^{3+}\text{-O}$ distances decreased and as the $\text{Fe}^{3+}\text{-O-Fe}^{3+}$ angle approached 180°. In the present study, attempts were made to estimate T_N as a function of vacancy concentration of the materials. For this purpose the following assumptions were made: (1) The $\text{Fe}^{3+}\text{-O}$ distance remains constant irrespective of the vacancy concentration; (2) the $\text{Fe}^{3+}\text{-O-Fe}^{3+}$ angle always maintains 180°; (3) La-ion deficiency gives no influence on T_N ; and (4) the oxygen and iron vacancies are randomly distributed. The existence of an oxygen ion vacancy may result in a decrease of one $\text{Fe}^{3+}\text{-O-Fe}^{3+}$ linkage, and the existence of an iron vacancy, three $\text{Fe}^{3+}\text{-O-Fe}^{3+}$ linkages. The T_N of LaFeO_3 without vacancies should be taken as 463°C (13). The results of the estimation of T_N for a series of materials are shown in Fig. 5, where line (I) is for the presence of only oxygen vacancies and line (II) is for the coexistence of both oxygen and iron vacancies. For specimen 1200, which has only

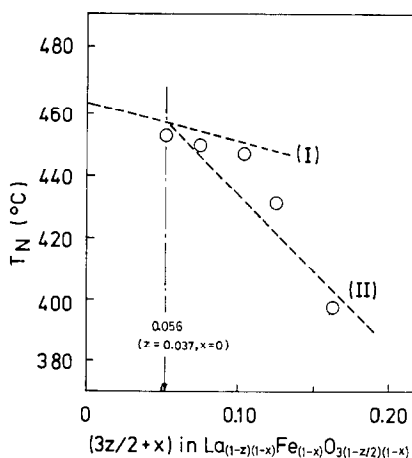


FIG. 5. Estimation of Néel temperature lowering due to (I) oxygen vacancy only and (II) both oxygen and iron vacancies and comparison with observed values.

oxygen vacancies accompanied by lanthanum deficiency ($z = 0.037$ and $x = 0.00$ in $\text{La}_{(1-z)(1-x)}\text{Fe}_{(1-x)}\text{O}_{3(1-z/2)(1-x)}$), the T_N value was estimated to be 457°C, which is close to the observed one, 453°C. Observed data points can be regarded as being along line (II). We can therefore say that the lowering in T_N is not satisfactorily explained by the presence of oxygen vacancies only, but by considering the presence of iron vacancies as well as oxygen vacancies. This fact also suggests that the vacancy model proposed for the materials in the present study is reasonable in the light of the magnetic data.

References

1. I. DZIALOSHINSKY, *J. Phys. Chem. Solids* **4**, 241 (1958).
2. T. MORIYA, "Magnetism," Vol. 1, p. 86, Academic Press, New York (1963); *Phys. Rev.* **120**, 91 (1960).
3. R. L. WHITE, *J. Appl. Phys.* **40**, 1061 (1969).
4. S. GELLER AND F. E. WOOD, *Acta Crystallogr.* **9**, 563 (1956).
5. W. C. KOEHLER AND E. O. WOLLAN, *J. Phys. Chem. Solids* **2**, 100 (1957).
6. K. P. BELOV, V. I. TVERONOVA, M. A. ZAITSEVA, A. M. KADOMTSEVA, A. A. KATANEL'SON, AND K. YATSKUL'YAK, *Sov. Phys.-Solid State* **6**, 80 (1964).

7. H. P. KLUG AND L. ALEXANDER, "X-ray Diffraction Procedures," p. 510, Wiley, New York (1954).
8. L. J. CABRI, *Amer. Mineral.* **54**, 539 (1969).
9. H. YAMAMURA AND R. KIRIYAMA, *Bull. Chem. Soc. Japan* **45**, 2702 (1972).
10. D. TREVES, *Phys. Rev.* **125**, 843 (1962); *J. Appl. Phys.* **36**, 1033 (1965).
11. M. A. GILLES, *Phys. Rev.* **109**, 777 (1958).
12. J. H. VAN VLECK, "The Theory of Electric and Magnetic Susceptibilities," Chap. XII, Oxford Univ. Press, New York (1932).
13. H. YAMAMURA, *Nippon Kagaku Kaishi* No. 12, 2231 (1972).